Italian Association of Aeronautics and Astronautics
XXV International Congress
9-12 September 2019 | Rome, Italy

NEIGHBORING OPTIMAL GUIDANCE AND PROPORTIONAL-DERIVATIVE ATTITUDE CONTROL APPLIED TO LOW-THRUST ORBIT TRANSFERS

M. Pontani[1*], F. Celani[2]

[1]Department of Astronautical, Electrical, and Energy Engineering – Sapienza University of Rome, via Salaria 851, 00138 Rome, Italy

[2]School of Aerospace Engineering – Sapienza University of Rome, via Salaria 851, 00138 Rome, Italy

*mauro.pontani@uniroma1.it, fabio.celani@uniroma1.it

ABSTRACT

This work presents a unified guidance and control architecture, termed VTD-NOG & PD-RM, and describes its application to low-thrust orbit transfer from a low Earth orbit to a geostationary orbit. The variable time-domain neighboring optimal guidance (VTD-NOG) is a feedback guidance technique based upon minimizing the second differential of the objective function along the perturbed trajectory, and was proven to avoid the numerical difficulties encountered with alternative neighboring optimal algorithms. VTD-NOG identifies the trajectory corrections assuming the thrust direction as the control input. A proportional-derivative attitude control based on rotation matrices (PD-RM) is used to drive the actual thrust direction toward the desired one, determined by VTD-NOG. Reaction wheels are employed to perform the attitude control action. In the dynamical simulations, thrust oscillations, errors on the initial conditions, and gravitational perturbations are considered. Extensive Monte Carlo simulations point out that orbit injection occurs with very satisfactory accuracy, even in the presence of nonnominal flight conditions.

Keywords: Low-thrust orbit transfers, neighboring optimal guidance, proportional-derivative attitude control

1 INTRODUCTION

Low-thrust propulsion is gaining an increasing use in space missions, due to its efficiency, related to high specific impulses. In fact, with regard to the overall propellant mass, low-thrust systems are proven to outperform high-thrust engines, in a wide variety of mission scenarios. However, deviations from the nominal trajectory related either to the imperfect modeling of the space vehicle or to unpredictable environmental conditions affect the real dynamics. Driving a spacecraft along a specified path thus requires defining the corrective actions aimed at compensating the nonnominal behavior due to these deviations, while minimizing the additional fuel required to perform the corrective maneuvers. Neighboring Optimal Guidance (NOG) is an implicit guidance concept that relies on the analytical second order optimality conditions, and assumes the minimum-time optimal transfer as the nominal trajectory. A common difficulty encountered in implementing NOG consists in the fact that the gain matrices become singular while approaching the final time. As a result, the real-time correction of the time of flight can lead to numerical difficulties so relevant to cause the failure of the guidance algorithm.

This research is focused on the original combination of two techniques applied to low-thrust orbit transfers, i.e. (i) the recently-introduced [1] variable-time-domain neighboring optimal guidance (VTD-NOG), and (ii) a proportional-derivative approach based on rotation matrices (PD-RM) as the attitude control algorithm. VTD-NOG belongs to the class of feedback implicit guidance approaches. A fundamental original feature of VTD-NOG is the use of a normalized time scale as the domain in which the nominal trajectory and the related vectors and matrices are defined. VTD-NOG identifies the trajectory corrections by assuming the thrust direction as the control input. Because the thrust direction is fixed with respect to the spacecraft, VTD-NOG iteratively generates the desired attitude, which can be eventually discontinuous across subsequent guidance intervals. This circumstance implies that the actual orientation, which is subject to the spacecraft attitude dynamics, does not coincide with the desired orientation. Hence, the attitude control system must be capable of maintaining the actual spacecraft orientation sufficiently close to the desired one. Reaction wheels are considered as the actuators that perform attitude control. The control law being adopted is proportional-derivative-like and uses directly the rotation matrices (PD-RM).
This study describes the application of VTD-NOG & PD-RM to the low-thrust orbit transfer that starts from a low Earth orbit (LEO) and ends at injection into a coplanar geostationary orbit (GEO). Several deviations from nominal flight conditions are assumed, i.e. (i) gravitational perturbations, (ii) errors on the initial conditions, and (iii) unpredictable oscillations of the propulsive thrust. They are being modeled in the context of extensive Monte Carlo simulations, with the final aim of proving that the unified architecture based on the joint use of VTD-NOG and PD-RM indeed represents an effective guidance and control approach, capable of determining precise and fuel-efficient low-thrust orbit transfers, in the presence of nonnominal flight conditions.

2 NOMINAL TRAJECTORY

This paper addresses the problem of driving a spacecraft from an equatorial circular low Earth orbit (LEO) at altitude of 400 km to a final, coplanar geostationary orbit (GEO), in the presence of nonnominal flight conditions. Both trajectory and attitude dynamics of the space vehicle are modeled. This section is devoted to defining the nominal transfer path. In this context, the space vehicle is modeled as a point mass. Subsequently, attitude dynamics is considered, with the final intent of determining the appropriate attitude control action.
Continuous low thrust propulsion is employed to perform the transfer at hand. Let c and n_0 denote the effective exhaust velocity of the propulsive system and the initial thrust acceleration. As the thrust magnitude is constant, the thrust acceleration is $a_T = n_0 c/(c - n_0 t)$, where t is the actual time. The following nominal values are assumed: $n_0 = 0.001 g_0$ and $c = 30$ km/sec $\left(g_0 = 9.8 \text{ m/sec}^2\right)$.

2.1 Formulation of the problem

The spacecraft motion can be described in the Earth-centered inertial frame, where $\hat{c}_1$ is the vernal axis and $\hat{c}_3$ points toward the Earth rotation axis. The two terminal orbits lie on the $(\hat{c}_1, \hat{c}_2)$-plane, i.e. the equatorial plane (cf. Fig. 1(a)). The time-varying position can be identified by the following three variables: radius r, absolute longitude ξ, and latitude ϕ. The spacecraft velocity can be projected into the rotating frame $(\hat{r}, \hat{t}, \hat{n})$, where $\hat{r}$ is aligned with the position vector $\boldsymbol{r}$ and $\hat{t}$ is parallel to the $(\hat{c}_1, \hat{c}_2)$-plane (and in the direction of the

spacecraft motion, cf. Fig 1(a)). The related components are denoted with (v_r, v_t, v_n) and termed respectively radial, transverse, and normal velocity component. The state vector $\boldsymbol{x}$ of the spacecraft includes the variables associated with the position and velocity vectors and is given by $\boldsymbol{x} := [r \quad \xi \quad \phi \quad v_r \quad v_t \quad v_n]^T$. The spacecraft is controlled through the thrust direction, defined by the in-plane angle α and the out-of-plane angle β, both illustrated in Fig. 1(b) (in which $\hat{T}$ is aligned with the thrust direction). Thus, the control vector is $\boldsymbol{u} := [u_1 \quad u_2]^T = [\alpha \quad \beta]^T$. The state equations govern the dynamics of the center of mass and are written in compact form as $d\boldsymbol{x}/dt = \tilde{\boldsymbol{f}}(\boldsymbol{x}, \boldsymbol{u}, t)$. The associated scalar equations [2], not reported for the sake of conciseness, include only the main gravitational term and the thrust acceleration as external actions, i.e. no perturbation is assumed. The boundary conditions correspond to terminal circular orbits, and can be written in compact form as $\boldsymbol{\psi}(\boldsymbol{x}_0, \boldsymbol{x}_f, t_f) = \boldsymbol{0}$. The problem at hand is then reformulated by using the dimensionless normalized time $\tau := t/t_f \quad (\Rightarrow \ \tau_0 \equiv 0 \le \tau \le 1 \equiv \tau_f)$, and the state equations are rewritten as $\dot{\boldsymbol{x}} = \boldsymbol{f}(\boldsymbol{x}, \boldsymbol{u}, t_f, t)$.

As the space vehicle uses continuous thrust, minimizing the propellant consumption is equivalent to minimizing the time of flight $(t_f - t_0)$. Thus, as t_0 is set to 0, the objective function is $J = t_f$.

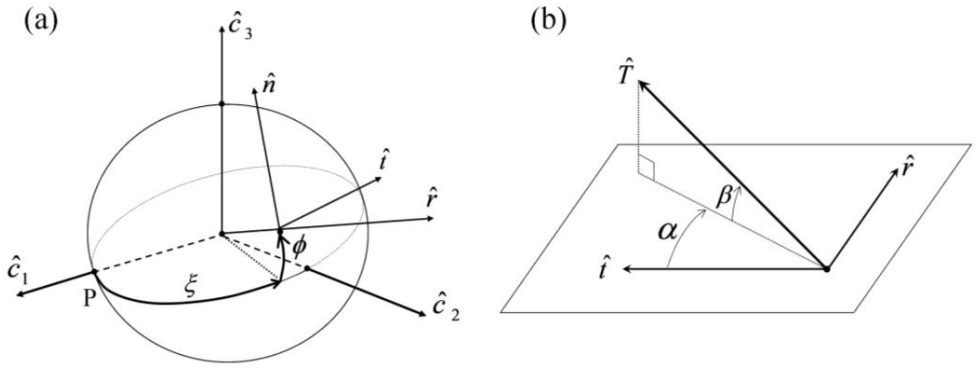

Figure 1: Reference frames (a) and thrust angles (b)

2.2 Minimum-time transfer trajectory

In order to state the necessary conditions for optimality, a Hamiltonian *H* and a function of the boundary conditions $\tilde{\Phi}$ are introduced as

$$H(\boldsymbol{x}, \boldsymbol{u}, t_f, \tau) := \boldsymbol{\lambda}^T \boldsymbol{f} \quad \text{and} \quad \tilde{\Phi}(\boldsymbol{x}_0, \boldsymbol{x}_f, t_f) := t_f + \boldsymbol{\upsilon}^T \boldsymbol{\psi} \tag{1}$$

where $\boldsymbol{\lambda}$ and $\boldsymbol{\upsilon}$ represent respectively the adjoint variable conjugate to the dynamics equations and to the boundary conditions. The set of the necessary conditions [3] include

- the adjoint equations for $\boldsymbol{\lambda}$, in conjunction with the respective boundary conditions,
- the Pontryagin minimum principle, leading to finding $\boldsymbol{u}$ in terms of $\boldsymbol{\lambda}$, and
- the transversality condition, which reduces to an inequality constraint.

In the formulation of the trajectory optimization problem the Earth gravitational field is assumed spherical. As no further external force affects the spacecraft motion and the terminal

orbits lie on the $(\hat{c}_1, \hat{c}_2)$-plane, the optimal transfer path can be assumed to lie on the $(\hat{c}_1, \hat{c}_2)$-plane as well. This means that $\phi = 0$, $v_n = 0$, and $\beta = 0$ along the optimal path. The latter is found through the indirect heuristic method [4], and the optimal time histories of the radius and thrust pointing angle are portrayed in Fig. 2.

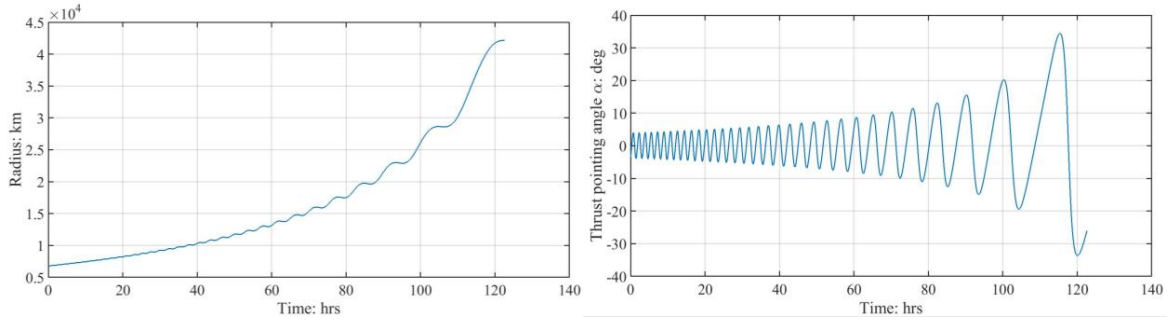

Figure 2: Radius (a) and thrust pointing angle (b) for the optimal transfer

3 VARIABLE-TIME-DOMAIN NEIGHBORING OPTIMAL GUIDANCE

Neighboring optimal guidance (NOG) belongs to the class of implicit guidance approaches and relies on the second-order sufficient conditions for optimality, in order to find the corrective control actions in the neighborhood of the reference trajectory. This is an optimal path that satisfies the second-order sufficient conditions for optimality.

This paper applies the variable-time-domain neighboring optimal guidance algorithm (VTD-NOG), described in full detail in Refs. 1 and 2, to the low-thrust orbit transfer of interest. VTD-NOG requires several offline steps, specifically

(a) determination of the optimal path, together with all the related quantities,
(b) numerical verification of the second-order sufficient conditions for optimality,
(c) integration of the modified sweep equations, to calculate the time-varying gain matrices, and
(d) interpolation of all the nominal quantities associated with the nominal (optimal) path.

Iterative real-time computations start at prescribed sampling times and are aimed at finding the control correction and the flight time update, such that the second differential of the objective function is minimized, while satisfying the first-order expansions of (a) the state equations, (b) the adjoint equations, (c) the parameter condition, and (d) the control condition. Novel features of VTD-NOG with respect to former NOG schemes are (i) the use of a variable time domain, (ii) new updating law for the time of flight, (iii) new termination criterion, and (iv) new sweep equations. These original features allow overcoming the main difficulties related to the use of former NOG schemes, in particular the occurrence of singularities in the gain matrices while approaching the final time and the lack of an efficient law for the iterative real-time update of the time of flight. These desirable characteristics are mainly related to the use of a normalized time domain τ, constrained to $[0,1]$. Figure 3 portrays a block diagram that illustrates the sample-data feedback structure of the VTD-NOG algorithm, in which the control and flight time corrections definitely depend on the state displacement $\delta \boldsymbol{x}$ (evaluated at specified discrete times) through the time-varying gain matrices, which are computed offline and stored onboard. The attitude control loop (encircled by the dotted line) is being outlined in the following.

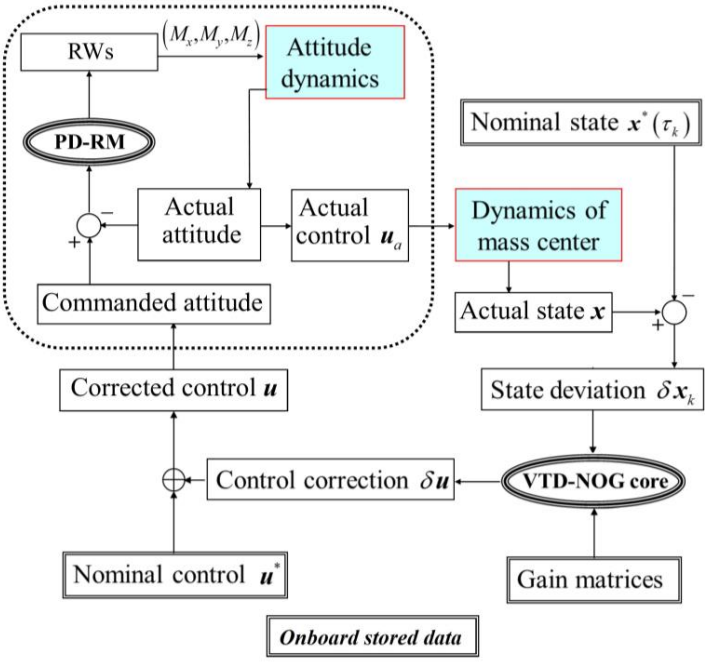

Figure 3: Block diagram of VTD-NOG & PD-RM

4 ATTITUDE CONTROL

With reference to Fig. 3, VTD-NOG yields the corrected control $\boldsymbol{u}$, i.e. the desired thrust direction. However, the actual thrust direction is aligned with the longitudinal axis of the spacecraft, and the spacecraft instantaneous orientation is associated with the body frame $(\hat{x}_b, \hat{y}_b, \hat{z}_b)$ where $\hat{x}_b$ is aligned with the longitudinal axis. Thus, $\boldsymbol{u}$ identifies the commanded direction of $\hat{x}_b$, denoted with $\hat{x}_b^{(c)}$. The remaining commanded unit vectors $\hat{y}_b^{(c)}$ and $\hat{z}_b^{(c)}$ are chosen so that in nominal flight conditions $\hat{z}_b^{(c)}$ lies in the equatorial plane and has positive component along the local nadir direction during the entire time of flight. Based on the latter choices, VTD-NOG determines unequivocally the commanded rotation matrix $\mathbf{R}_c$, which relates $(\hat{c}_1, \hat{c}_2, \hat{c}_3)$ to $\left(\hat{x}_b^{(c)}, \hat{y}_b^{(c)}, \hat{z}_b^{(c)}\right)$.

To enforce convergence of the actual attitude, represented by rotation matrix $\mathbf{R}$, toward the commanded attitude, represented by rotation matrix $\mathbf{R}_c$, the following PD-like attitude control action is applied [5]:

$$\boldsymbol{M}_c = -\mathbf{K}_p \sum_{i=1}^{3} \left(\boldsymbol{e}_i \times \mathbf{R}_c \mathbf{R}^T \boldsymbol{e}_i \right) - \mathbf{K}_d \boldsymbol{\omega} \tag{2}$$

In the previous equation $\boldsymbol{M}_c$ are the body coordinates of the control torque generated by the reaction wheel assembly, $\mathbf{K}_p = \mathrm{diag}\{k_{px}, k_{py}, k_{pz}\}$ and $\mathbf{K}_d = \mathrm{diag}\{k_{dx}, k_{dy}, k_{dz}\}$ are positive control gains, $\{\boldsymbol{e}_i\}_{i=1,2,3}$ form the 3 by 3 identity matrix $[\boldsymbol{e}_1 \quad \boldsymbol{e}_2 \quad \boldsymbol{e}_3]$, and $\boldsymbol{\omega}$ are the body coordinates of the spacecraft angular velocity with respect to $(\hat{c}_1, \hat{c}_2, \hat{c}_3)$.

5 VTD-NOG & PD-RM APPLIED TO LEO-GEO TRANSFER

During the orbit transfer, the spacecraft is affected by the Earth gravitational field. However, the Earth gravitational potential differs to some extent from that generated by a spherical mass distribuition. As a result, some significant harmonics of the Earth gravitational potential [6] are to be included in the dynamical model, in order to yield more realistic results from simulations. Thus, all the harmonics with magnitude $|J_{lm}| > 10^{-6}$ are included in the dynamical simulations, i.e. J_2 J_3, J_4, J_{22}, and J_{31}. Moreover, also the gravitational perturbations due to Moon and Sun as third bodies [6] must be taken into account.

The spacecraft has initial mass $\tilde{m}_0 = 2400$ kg and maximal torque generated by the reaction wheels about each body axis $\overline{M_x} = \overline{M_y} = \overline{M_z} = 0.5$ N m, whereas the time-varying inertia moments I_x, I_y, and I_z are governed by

$$I_x = I_{x0} + \dot{I}_x t, \quad I_y = I_{y0} + \dot{I}_y t, \quad I_z = I_{z0} + \dot{I}_z t \tag{3}$$

where $I_{x0} = 1200$ kg m^2, $\dot{I}_x = -3.92 \cdot 10^{-4}$ kg m^2/sec, $I_{y0} = I_{y0} = 800$ kg m^2, and $\dot{I}_y = \dot{I}_z = -2.61 \cdot 10^{-4}$ kg m^2/sec). Moreover, the following values are selected for VTD-NOG & PD-RM. The sampling interval Δt_S is set to 15 min, whereas the control gains are selected using a trial and error approach, and set to the following values: $k_{px} = 11.76$, $k_{dx} = 151.2$, $k_{py} = k_{py} = 7.84$, $k_{dy} = k_{dz} = 100.8$.

Another reason for the existence of deviations from nominal flight conditions is related to the fact that the commanded attitude does not coincide with the actual attitude. This circumstance is pointed out also in Fig. 3, which illustrates clearly that the corrected control $\boldsymbol{u}$ does not coincide with the actual control $\boldsymbol{u}_a$, which affects the real dynamics of the center of mass.

Moreover, for the initial conditions errors on the initial radius and latitude are assumed, with Gaussian distribution, zero mean value and standard deviation $r_0^{(\sigma)}$ (for r_0) and $\phi_0^{(\sigma)}$ (for ϕ_0) equal to 10 km and 0.085 deg, respectively. The latter value correspond to an out-of-plane displacement of 10 km. Moreover, displacements for the velocity components are simulated as well. Specifically, a velocity magnitude displacement with zero mean value and standard deviation $v_0^{(\sigma)} = 30$ m/sec is assumed, while the velocity direction has uniform distribution over a unit sphere. A different approach is chosen for the perturbation of the thrust acceleration. In fact, usually the thrust acceleration exhibits small fluctuations. If t_f^* denotes the optimal time of flight, this behavior is modeled through a trigonometric series,

$$n_0^p = n_0 \left\lfloor 1 + \sum_{k=1}^{5} \tilde{a}_k \sin\left(\frac{2k\pi t}{t_f^*}\right) + \sum_{k=1}^{5} \tilde{a}_{k+5} \cos\left(\frac{2k\pi t}{t_f^*}\right) \right\rfloor \tag{4}$$

The coefficients $\{\tilde{a}_k\}_{k=1,\ldots,10}$ have a random Gaussian distribution centered around the zero and a standard deviation equal to 0.01. At the end of VTD-NOG & PD-RM, two statistical quantities are evaluated, i.e. the mean value and the standard deviation for all of the outputs of interest. In Table 1, which summarizes the statistics based on 100 Monte Carlo simulations, the symbols $\overline{\Delta\chi}$ and $\chi^{(\sigma)}$ denote the mean error (with respect to the nominal value) and

standard deviation of χ henceforth. Figure 4 portrays the time histories of the state and control torques obtained in the Monte Carlo campaign. The numerical results prove that VTD-NOG & PD-RM yields excellent results in terms of accuracy at orbit injection, with only modest displacements of the perturbed times of flight with respect to the nominal value.

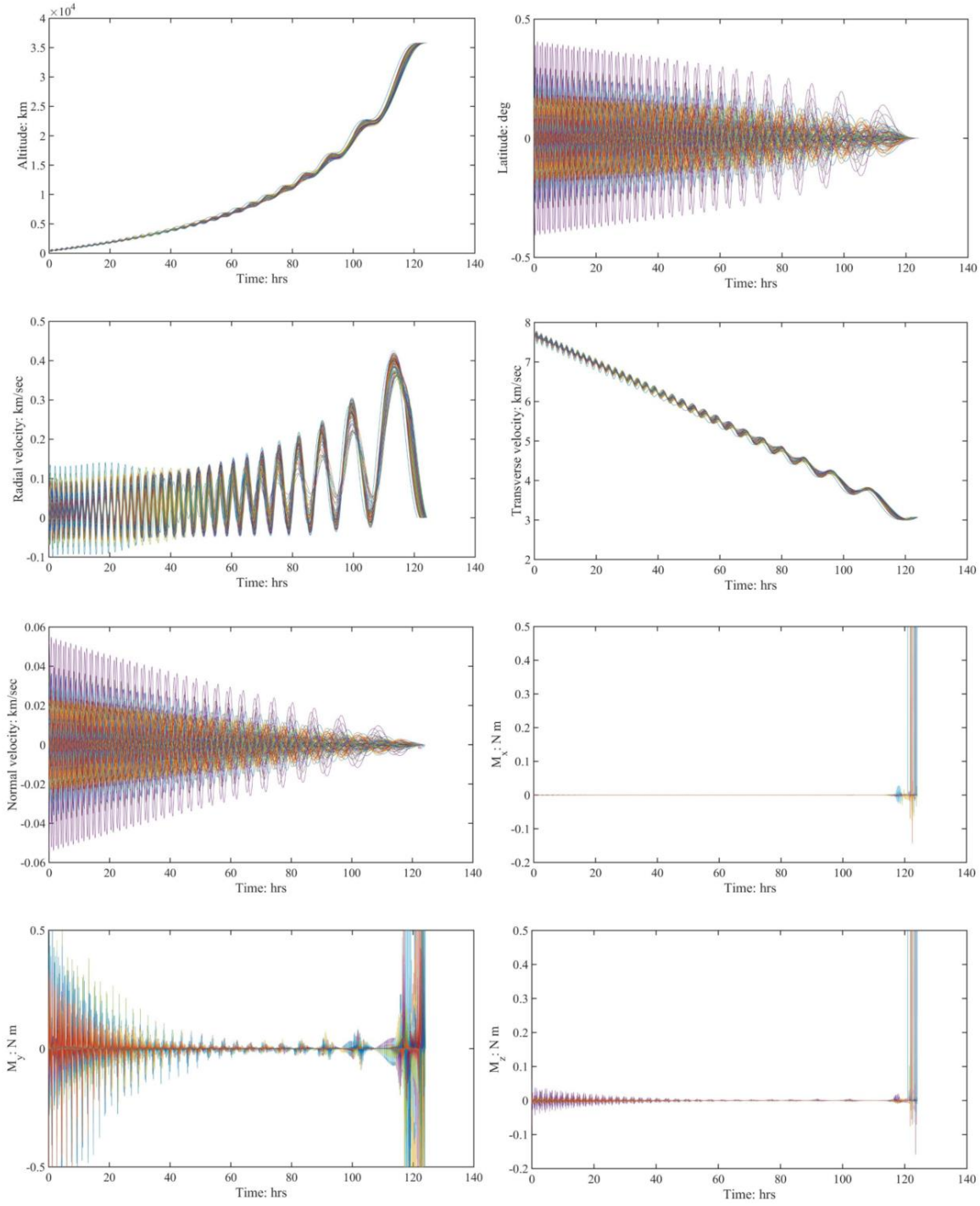

Figure 4: State and attitude control along perturbed paths

$\overline{\Delta r_f}$ (km)	$\overline{\Delta\phi_f}$ (deg)	$\overline{\Delta v_{rf}}$ (m/sec)	$\overline{\Delta v_{tf}}$ (m/sec)	$\overline{\Delta v_{nf}}$ (m/sec)	$\overline{t_f}$ (sec)
−0.98	–6.6 e –5	0.346	−1.410	−0.401	122.84
$r_f^{(\sigma)}$ (km)	$\phi_f^{(\sigma)}$ (deg)	$v_{rf}^{(\sigma)}$ (m/sec)	$v_{tf}^{(\sigma)}$ (m/sec)	$v_{nf}^{(\sigma)}$ (m/sec)	$t_f^{(\sigma)}$ (sec)
0.263	1.2e –4	0.716	1.156	0.618	0.53

Table 1: Statistics based on the outputs of the Monte Carlo campaign ($\overline{\Delta\chi_f}$ = mean value of the error on the desired final value of χ ; $\chi_f^{(\sigma)}$= standard deviation of the final value of χ ; $\overline{t_f}$ = mean value of the time of flight; $t_f^{(\sigma)}$ = standard deviation of the time of flight)

6 CONCLUDING REMARKS

This work outlines and applies VTD-NOG & PD-RM, a new, general-purpose guidance and control algorithm for space vehicles, The variable-time-domain neighboring optimal guidance (VTD-NOG) is a feedback guidance technique based upon minimizing the second differential of the objective function along the perturbed trajectory. Due to adoption of a normalized time scale as the domain in which the nominal trajectory is defined, the gain matrices remain finite for the entire time of flight, while the updating law for the time of flight and the termination criterion find consistent definitions. A proportional-derivative approach using rotation matrices (PD-RM) is employed in order to drive the actual spacecraft orientation toward the desired one. The new guidance and control architecture based on the joint use of VTD-NOG & PD-RM is applied to a LEO-to-GEO transfer, in the presence of oscillating perturbations of the propulsive thrust, errors on the initial conditions, and gravitational perturbations. Extensive Monte Carlo simulations point out that orbit injection at GEO occurs with very satisfactory accuracy even in the presence of nonnominal flight conditions, at the price of modest variations of the time of flight.

REFERENCES

[1] M. Pontani, G. Cecchetti, P. Teofilatto. Variable-Time-Domain Neighboring Optimal Guidance, Part 1: Algorithm Structure. *Journal of Optimization Theory and Applications*, Vol. 166, No. 1, pp. 76-92 (2015).

[2] M. Pontani, F. Celani. Neighboring optimal guidance and constrained attitude control applied to three-dimensional lunar ascent and orbit injection. *Acta Astronautica*, Vol. 156, pp. 78-91 (2019).

[3] D. G. Hull. *Optimal Control Theory for Applications*. Springer International Edition, New York, NY, pp. 199-254 (2003).

[4] M. Pontani, B. A. Conway. Minimum-Fuel Finite-Thrust Relative Orbit Maneuvers via Indirect Heuristic Method. *Journal of Guidance, Control, and Dynamics*, Vol. 38, No. 5, pp. 913-924 (2015).

[5] N. A. Chaturvedi, A. K. Sanyal, N. H. McClamroch. Rigid-Body Attitude Control. *IEEE Control Systems*, Vol. 31, No. 3, pp. 30-51 (2011).

[6] H. Schaub, J. L. Junkins. *Analytical Mechanics of Space Systems*. AIAA Education Series, Reston, VA, pp. 545-556, (2009).